

# A Tetratricopeptide Repeat Half-Site in the Aryl Hydrocarbon Receptor Is Important for DNA Binding and *trans*-Activation Potential

STEVEN L. LEVINE, JOHN R. PETRULIS, ALLISON DUBIL, and GARY H. PERDEW

Center for Molecular Toxicology and Carcinogenesis, Department of Veterinary Science, The Pennsylvania State University, University Park, Pennsylvania

Received July 11, 2000; accepted September 12, 2000

This paper is available online at <http://www.molpharm.org>

## ABSTRACT

Similar to certain unliganded steroid hormone receptor complexes, the unliganded aryl hydrocarbon receptor has been shown to consist of a multimeric core complex that includes the 90-kDa heat shock protein (hsp90) and the immunophilin-like hepatitis B X-associated protein 2 (XAP2). Immunophilins and XAP2 associated with these complexes bind to the carboxyl-terminal end of hsp90 through an interaction with their tetratricopeptide repeat (TPR) domains. The consensus TPR binding motif contains two domains, A and B. Recently, the carboxyl terminus of XAP2 has been shown to contain a highly conserved TPR domain that is required for the assembly of XAP2 with both hsp90 and AhR. A search of the murine AhR sequence identified domain B (A-F-A-P) of the consensus TPR sequence directly adjacent to the carboxyl-terminal side of the helix-loop-helix region of the murine and human AhR. We hypothesized that this conserved domain B region may be involved with mediating interactions between either AhR-hsp90,

AhR-XAP2, and/or AhR-AhR nuclear translocator protein. Site-directed mutagenesis of the amino-terminal alanine residue of this region to an aspartic acid (A78D) completely inhibited 2,3,7,8-tetrachloro-*p*-dioxin (TCDD)-dependent activation of a xenobiotic response element (XRE) driven gene expression construct in transfected COS-1 and BP8 cells. The A82F mutation caused a 40 to 50% decrease in TCDD-dependent activation. The inability of A78D and the reduction of A82F to *trans*-activate XRE-driven reporter activity did not result from impaired AhR-XAP2-hsp90 interactions, TCDD-dependent AhR translocation to the nucleus, or AhR-AhR nuclear translocator protein interactions. In vitro DNA binding analysis demonstrated that loss of *trans*-activation potential by the A78D mutation resulted from impaired XRE binding. This study underscores the potential importance of AhR mutations that occur naturally outside of known functional domains.

Many of the biochemical and toxic effects of HAHs and PAHs seem to be mediated through cytoplasmic binding to the aryl hydrocarbon receptor (Whitlock, 1987). In its inactive form, the aryl hydrocarbon receptor (AhR) resides in the cytoplasm in a tetrameric 9S core complex consisting of the AhR, a dimer of hsp90 (Perdew, 1988) and XAP2 (Carver and Bradfield, 1997; Ma and Whitlock, 1997; Meyer et al., 1998). After ligand activation, the AhR *trans*-locates to the nucleus where it dimerizes with the ARNT protein (Reyes et al., 1992; Hord and Perdew, 1994). Activation of transcription by the

AhR is best understood for the *CYP1A1* gene. *CYP1A1* gene activation results from an interaction of the AhR-ARNT dimer with several copies of short sequences, termed xenobiotic response elements (XREs), located in the 5'-flanking region of the gene (Denison et al., 1989). The hydroxylase activity of *CYP1A1* metabolizes PAHs, such as benzo[a]pyrene, to cytotoxic as well as carcinogenic products.

Investigations with the use of deletion mutants and site-directed mutagenesis have identified functional domains within the AhR and the ARNT proteins. The PAS-domain of the AhR contains a nuclear export signal domain and both AhR and ARNT contain nuclear localization signals (Eguchi et al., 1997; Ikuta et al., 1998). In addition, both the AhR and ARNT contain basic HLH motifs toward their amino termini

This work was supported by the National Institute of Environmental Health Sciences (NIEHS) Grant ES04869 (G.P.) and an NIEHS Postdoctoral Fellowship (S.L.).

**ABBREVIATIONS:** HAHs, halogenated aromatic hydrocarbons; PAHs, polycyclic aromatic hydrocarbons; AhR, aryl hydrocarbon receptor; hsp90, 90-kDa heat-shock protein; XAP2, hepatitis B virus X-associated protein 2; ARNT, aryl hydrocarbon receptor nuclear translocator; XRE, xenobiotic response element; HLH, helix-loop-helix; PAS, PER-ARNT-SIM (periodicity/aryl hydrocarbon receptor nuclear translocator/simple-minded); TPR, tetratricopeptide repeat; mAhR, murine aryl hydrocarbon receptor; CHAPS, 3-[[3-(cholamidopropyl)dimethylammonio]-1-propanesulfonate]; PVDF, polyvinylidene difluoride; TBE, Tris-borate-EDTA; MOPS, 4-morpholinepropanesulfonic acid; MENG, MOPS/EDTA/Na<sub>3</sub>/glycerol; Tricine, N-[2-hydroxy-1,1-bis(hydroxymethyl)ethyl]glycine; PAGE, polyacrylamide gel electrophoresis; mAb, monoclonal antibody; RLUs, relative light units; DMSO, dimethyl sulfoxide; TCDD, 2,3,7,8-tetrachlorodibenzo-*p*-dioxin; CDTA, *trans*-1,2-diaminocyclohexane-*N,N,N',N'*-tetraacetic acid.

(Schmidt et al., 1996). The HLH region participates in dimerization with ARNT and the basic regions allow the AhR-ARNT heterodimer to bind XREs (Dolwick et al., 1993; Fukunaga et al., 1995; Dong et al., 1996). Near the center of both proteins is a PAS homology region of approximately 300 amino acids that contains two degenerate direct repeats of approximately 50 amino acids, identified as PAS A and PAS B. The hsp90 contacts two regions of the AhR, including the PAS region and the basic HLH region (Perdew and Bradfield, 1996). The PAS domains of both proteins also participate in AhR-ARNT dimerization. The PAS B of AhR contains, at least in part, the ligand binding domain (Burbach et al., 1992). The carboxyl-terminal half of AhR and ARNT contain a *trans*-activation domain that mediates transcriptional activation (Whitelaw et al., 1994; Sogawa et al., 1995).

In a similar manner to the inactive AhR complex, steroid hormone receptors consist of a multimeric complex. These complexes contain a ligand-binding subunit on the receptor, a dimer of hsp90, p23, and an immunophilin. The immunophilins associated with these complexes bind to the carboxyl-terminal end of hsp90 by their tetratricopeptide repeat (TPR) domains. The TPR is a degenerate 34-amino-acid motif that is widespread throughout evolution (i.e., it appeared early in evolution) (Goebel and Yanagida, 1991). Functionally, TPR mediated protein-protein interactions are involved in cell cycle control, transcriptional repression, stress response, protein kinase inhibition, mitochondrial and peroxisomal protein transport, and neurogenesis (Goebel and Yanagida, 1991). Recently, the carboxyl terminus of XAP2 has been shown to contain a highly conserved TPR domain. This TPR domain is required for the assembly of XAP2 with hsp90 and the AhR (Meyer and Perdew, 1999). Although the complete role of XAP2 in the unliganded AhR complex is unknown, XAP2 has been shown to enhance cytosolic AhR levels and transactivation potential (Ma and Whitlock, 1997; Meyer and Perdew, 1999; LaPres et al., 2000).

The TPR consensus sequence is composed of two domains, A (W-LG-Y) and B (A-F-A-P), which are conserved in terms of their size, hydrophobicity, and spacing. The two TPR subdomains have a high probability of forming amphipathic  $\alpha$ -helices, which are proposed to associate with another protein (Lamb et al., 1995). This association results from domain A forming a hydrophobic pocket, allowing the large side chain of the phenylalanine in domain B to fit into the pocket (Hirano et al., 1990; Sikorski et al., 1993). To date, evidence for direct TPR-TPR mediated protein-protein interactions has not been reported; however, TPR-containing proteins have been shown to form complexes (Lamb et al., 1994). Interestingly, the murine and human AhRs contain the signature residues found in domain B of the TPR. This purported half-site for a TPR domain is located between residues 78 and 90 of both the murine and human AhR proteins. Figure 1 compares the purported domain B of the TPR half-site found in both the human and the murine AhR along with the TPR domain found in XAP2 relative to the consensus TPR domain. A recent examination of the functional role of TPR domain B within XAP2 revealed that changing conserved residues in domain B disrupted the interaction with the AhR-hsp90 complex in COS-1 cells (Meyer et al., 2000). The aim of this study was to characterize the functional role of conserved amino acids within the region representing do-

main B of a TPR in the murine AhR and in AhR-ARNT mediated signal transduction.

## Experimental Procedures

**Materials.** Fetal bovine serum was purchased from Hyclone Labs (Logan, UT). Acrylamide and ammonium persulfate were purchased from Fisher (Pittsburgh, PA). [ $\gamma$ - $^{32}$ P]ATP (6000 Ci/mmol) and goat anti-mouse  $^{125}$ I-IgG was purchased from New England Nuclear (Boston, MA). Oligonucleotides for polymerase chain amplifications were purchased from Operon (Alameda, CA). LipofectAMINE reagent, opti-MEM, and *Escherichia coli* DH5 $\alpha$  were purchased from Life Technologies (Gaithersburg, MD). COS-1 cells were purchased from the American Type Culture Collection (Manassas, VA). SDS was purchased from Bio-Rad (Hercules, CA). Tricine, glycine, Tris, and CHAPS were purchased from Research Organics (Cleveland, OH). The luciferase assay system was purchased from Promega (Madison, WI). BCA protein assay reagents were purchased from Pierce (Rockford, IL). TNT T7 coupled reticulocyte system was purchased from Promega. [ $^{35}$ S]methionine was purchased from Amersham (Buckinghamshire, UK). PVDF Immobilon-P was purchased from Millipore (Bedford, MA). DNA retardation gels and high-density TBE sample buffer was purchased from Novex (Carlsbad, CA). pEYFP-N1 yellow fluorescent protein vector was purchased from CLONTECH Laboratories, Inc. (Palo Alto, CA). Vectashield mounting medium was purchased from Vector Laboratories Inc. (Burlingame, CA). All other materials were purchased from Sigma (St. Louis, MO).

**Site-Directed Mutagenesis.** Site-directed mutagenesis of pcDNA3/ $\beta$ mAHR (Fukunaga and Hankinson, 1996) was performed using Stratagene's Quick Change site-directed mutagenesis procedure, according to the manufacturers instructions (Stratagene, Palo Alto, CA). The proposed TPR half-site is located between amino acids 79 and 90 in the mouse AhR. The mutations included changing the alanine at position 78 to an aspartic acid, changing the phenylalanine at position 82 to an alanine, and a double mutant that included both mutations. These amino acid changes are illustrated in Fig. 1. All AhR constructs were sequenced to confirm the presence of only the targeted base changes at the DNA Core Facility at the Pennsylvania State University.

**Examination of AhR-hsp90-XAP2 Interactions in COS-1 Cells.** COS-1 cells were transiently transfected (80% confluent) in 10-cm<sup>2</sup> plates with either 6  $\mu$ g of wild-type pcDNA3/ $\beta$ AhR or a mutant pcDNA3/ $\beta$ AhR and 3  $\mu$ g of pCI/XAP2 (Meyer et al., 1998). Control transfections contained 6  $\mu$ g of empty pcDNA3 vector and 3  $\mu$ g of empty pCI vector using the LipofectAMINE procedure. Transfected COS-1 cells were removed from the transfection plates with trypsin-EDTA 36 h after transfection and were lysed in 200  $\mu$ L

A78D	VINKLDKLSVLRLSVTYLRDKSFFDVALKSTPAD
F82A	VINKLDKLSVLRLSVTYLRAKSFADVALKSTPAD
A78D:F82A	VINKLDKLSVLRLSVTYLRDKSFFADVALKSTPAD
mAhR	VINKLDKLSVLRLSVSYLRAKSFDFDVALKSTPAD
hAhR	VINKLDKLSVLRLSVTYLRAKSFDFDVALKSTPAD
XAP2	VKAYFKRGKAHAHVWNAQEAQADFAKVIELDPAL
TPR	
CONSENSUS	...W..LG.....Y....A...F...A....P..
	Domain A Domain B

**Fig. 1.** Schematic representation of the amino acid mutations made to the murine AhR. The black boxes in the first three lines indicate amino acid substitutions in the respective mutant; In the next three lines, black boxes indicate amino acid residues that are not conserved between the murine AhR (mAHR), human AhR, and XAP2. Domains A and B of the tetratricopeptide consensus sequence are aligned with the mAHR, human AhR, and XAP2 sequence. The TPR consensus was generated from CD16, CD23, CDC27, SSN6, and SK13 (Lamb et al., 1995).

MENG buffer (25 mM MOPS, 2 mM EDTA, 0.02% NaN<sub>3</sub>, 10% glycerol, pH 7.4), 1% Nonidet P-40, containing 1× protease inhibitor cocktail (Sigma) over 15 min on ice with vortexing. Cell lysates were centrifuged at 105,000g for 1 h in a Beckman 70Ti rotor (Beckman Instruments, Pal Alto, CA). To immunoprecipitate AhR-hsp90-XAP2 complexes, 5 µg of AhR specific mAb RPT9 (Perdew et al., 1995) was bound to a 25-µL packed bed volume of anti-mouse IgG agarose in MENG over 1 h on ice. The resin was washed three times in MENG and once in the buffer containing MENG, 20 mM sodium molybdate, 2 mg/ml BSA, and 2 mg/ml ovalbumin (IPMAO buffer). The cell lysate was added to the RPT9 agarose in a total volume of 1 ml in IPMAO buffer and immunoprecipitated on ice for 1 h. The bound mAhR complexes were washed once in IPMAO buffer and then washed four times in MENG containing 20 mM sodium molybdate. An equal volume of 2× Tricine sample buffer was added to the agarose, samples were heated at 95°C for 5 min, and resolved by SDS-PAGE on an 8% Tricine gel for 3 h at 30 V, followed by 18 h at 60 V. After electrophoresis, the proteins were transferred to a PVDF membrane. Transfers were performed at 15 V for 3 h in a Genie electroblot unit (Idea Scientific, Minneapolis, MN) in transfer buffer [20 mM Tris, 185 mM glycine, 20% (v/v) methanol] and the membrane was blocked for 1 h in a buffer containing 3% (w/v) BSA in PBS containing 10 mM Na<sub>2</sub>HPO<sub>4</sub>, 0.05% (v/v) Tween 20, pH 7.4 at 25°C. The membrane was rinsed once in blot wash buffer consisting of 0.1% (w/v) BSA in PBS containing 0.5% (v/v) Tween 20. The AhR-specific mAb RPT1 was used to detect the wild-type AhR protein and mutant AhR proteins (Perdew et al., 1995), the anti-hsp84/86 rabbit polyclonal antibodies were used to detect hsp90 (Perdew et al., 1993), and the rabbit polyclonal anti-XAP2 antibody provided by E. Croze (Berlex Laboratories, Richmond, CA) was used to detect XAP2. Blots were incubated with either mAb RPT1, anti-hsp84/86 rabbit polyclonal antibodies, or with an anti-XAP2 antibody at a dilution of 1:1000 in wash buffer at 25°C for 1 h. After five 10-min rinses in wash buffer, bound antibodies were detected with either 1 µCi/ml <sup>125</sup>I-sheep-anti-mouse IgG or 1 µCi/ml [<sup>125</sup>I]-donkey-anti-rabbit IgG for 1 h at 25°C, followed by 5 × 10 min rinses in wash buffer. <sup>125</sup>I-sheep-anti-mouse IgG and <sup>125</sup>I-donkey-anti-rabbit IgG blots were visualized using a Bio-Rad GS-363 Molecular Imager System PhosphorImager.

**In Vitro Protein Expression, Dimerization, and Immunoprecipitation.** AhR cDNAs were transcribed/translated in the TNT T7 coupled reticulocyte system (Promega) in the presence of [<sup>35</sup>S]methionine, whereas pcDNA3/mARNT/FLAG (Tsai and Perdew, 1997) was translated in the absence of isotope. AhR and mutant AhR proteins were mixed with pcDNA3/mARNT/FLAG, in equimolar amounts, in the presence or absence of 20 nM TCDD and incubated at 30°C for 2 h. The AhR-ARNT mixture was immunoprecipitated with 25 µL of anti-FLAG M2 affinity gel. The final buffer composition during immunoprecipitation contained MENG containing 20 mM sodium molybdate, 150 mM NaCl, and 1× protease inhibitor cocktail. For control experiments, the anti-FLAG M2 affinity gel was preincubated over night with 90 nmol of the FLAG peptide (DYKDDK) on ice before the AhR-ARNT translation mixture was incubated with the blocked anti-FLAG M2 affinity gel. Immunoprecipitations were incubated for 1 h on ice. The immunoprecipitations were washed three times with 1 ml of MENG containing 300 mM NaCl, 0.5% CHAPS and then washed twice with MENG before SDS-PAGE on an 8% Tricine gel. The proteins were transferred to a PVDF membrane at 15 V for 3 h in a Genie Blotting unit. PhosphorImaging of the membrane was performed using a Packard Cyclone PhosphorImager (Meriden, CT) and quantification was conducted with Packard Optiquant Image Analysis Software. Mean values were calculated from three independent experiments.

**Luciferase Reporter Gene Assay.** The potential of transiently transfected mutant AhRs to activate XRE-driven luciferase activity were compared in COS-1 cells and BP8 cells using the LipofectAMINE procedure. COS-1 cells (80% confluent) in six-well plates were cotransfected with 50 ng of either wild-type pcDNA3/βmAhR or

pcDNA3/βmAhR mutants, 100 ng of pGudLuc6.1, 100 ng of pSV-β-galactosidase, and equalized to 1.5 µg of total DNA with 1.25 µg of pcDNA3. Control transfections contained 100 ng of pGudLuc6.1, 100 ng of pSV-β-galactosidase, and equalized to 1.5 µg of total DNA with 1.3 µg of pcDNA3. BP-8 cells (80% confluent) in six-well plates were cotransfected with 50 ng of either wild-type pcDNA3/βmAhR or mutant pcDNA3/βmAhR, 100 ng of pGudLuc6.1, and equalized to 1.5 µg with 1.35 µg of empty pcDNA3. Control transfections contained 100 ng of pGudLuc6.1, 100 ng of pSV-β-galactosidase, and were equalized to 1.5 µg of total DNA with 1.3 µg of pcDNA3. Twenty-four hours after transfection, cells were then incubated with either DMSO (1 µL/ml) or 10 nM TCDD (1 µL/ml) for 8 h. At the end of the exposure period, cells were lysed in 25 mM Tris-phosphate/2 mM dithiothreitol/2 mM CDTA/10% glycerol/1% Triton X-100 and assayed for luciferase activity using the Promega luciferase assay system according to the manufacturer's instructions. Luciferase activity was measured in a Turner model 20e luminometer (Sunnyvale, CA) and luciferase activity is expressed as RLUs. Luciferase activity was normalized to β-galactosidase activity in COS-1 cells and protein levels in BP8 cells. Protein levels in BP8 cells were measured with the BCA protein assay.

**Quantitative Western Blot Analysis of AhR.** To assess the expression of wild-type and mutant AhR cDNAs, COS-1 cells plated into 10-cm<sup>2</sup> culture dishes (80% confluent), and transfected with 0.5 µg of either wild-type or mutant pcDNA3/βmAhR cDNAs and 8.5 µg of pcDNA3 using the LipofectAMINE procedure. Cells were harvested with trypsin-EDTA 36 h after transfection, were lysed in MENG containing 1% Nonidet P-40, were vortexed, and were incubated over 15 min on ice with vortexing. Cell lysates were centrifuged for 1 h at 105,000g and cytosolic protein levels were measured with the bicinchoninic acid protein assay. One hundred micrograms of cytosol was mixed with an equal volume of 2× Tricine sample buffer, heated at 95°C for 5 min and resolved by SDS-PAGE on an 8% Tricine gel. After electrophoresis, the proteins were transferred to a PVDF membrane. The membrane was blocked as described previously and incubated with the anti-AhR mAb RPT1 at a dilution of 1:1000 and anti-p50 (mcdc37) mAb C1p50 (Perdew et al., 1997) for 1 h in wash buffer at 25°C. The anti-p50 mAb was used as a loading control for normalization of AhR protein levels. The blot was rinsed 5 × 10 min with wash buffer and incubated for 1 h in wash buffer containing 1 µCi/ml <sup>125</sup>I-sheep-anti-mouse IgG. The blot was rinsed 5 × 10 min in wash buffer and PhosphorImaged with a Bio-Rad GS-363 Molecular Imager System. AhR levels and p50 levels were quantified with the Bio-Rad Molecular Analyst software version 1.4.

**In Vitro DNA Binding.** XRE binding assays were performed with in vitro transcribed/translated pcDNA3/mAhR and pcDNA3/mARNT in the TNT T7 coupled reticulocyte system in the absence of isotope. Wild-type AhR and mutant AhR translations were mixed with pcDNA3/mARNT for dimerization, in equimolar amounts, in the presence or absence of 20 mM TCDD, and incubated at room temperature for 15 min. Four microliters from each AhR-ARNT mixture was added to a mixture of 25 mM HEPES, pH 7.5, 10% (v/v) glycerol, 10 mM KCl, 540 ng of poly(dI:dC), 5 mM dithiothreitol, and 4 mM MgCl<sub>2</sub>, 2.5% CHAPS in a 25 µL assay volume. The mixture was incubated at room temperature for 15 min followed by addition of 0.5 ng of <sup>32</sup>P-labeled oligonucleotide (DRE) (provided by M. Denison, University of California, Davis, CA), and incubated for another 15 min at room temperature. The purified oligonucleotides were radiolabeled with [<sup>γ</sup>-<sup>32</sup>P]ATP as described by Denison et al. (1988). After addition of 5 µL of Hi-Density TBE Sample Buffer to the reaction mixture, preparations were separated by electrophoresis on a 6% nondenaturing polyacrylamide gel at 10 mA using 0.5× TBE buffer. The specificity of DRE binding by the AhR:ARNT heterodimer was assessed by using in vitro transcribed/translated AhR alone in the presence of 20 mM TCDD. Mean values were calculated from four independent experiments. Dried gels were PhosphorImager with a Bio-Rad GS-363 Molecular Imager System.



**AhR Translocation Analysis and Functionality of AhR-YFP cDNAs in COS-1 cells.** COS-1 cells were grown on glass cover slips in six-well culture dishes were transfected with 1  $\mu$ g pCI-XAP2 and 0.5  $\mu$ g AhR-YFP fusion construct using LipofectAMINE according to the manufacturer's instructions. Twenty-four hours after transfection, cells were rinsed twice with PBS, fixed for 15 min in 4% formaldehyde/PBS at room temperature, rinsed twice with PBS, and the inverted cover slips mounted onto microscope slides with Vectashield mounting medium. Visualization and fluorescence micrographs were obtained with a SPOT SP100 cooled CCD camera fitted to a Nikon Optiphot-2 upright microscope with EFD-3 episcopic fluorescence attachment using a Nikon Pan Fluor 100 $\times$  oil immersion objective.

The potential of transiently transfected mutant AhR-YFP cDNAs to activate XRE-driven luciferase activity was examined in COS-1 cells using the LipofectAMINE procedure. COS-1 cells (80% confluent) in six-well plates were cotransfected with 50 ng of either wild-type pEYFP-N1/mAhR-YFP or mutant pEYFP-N1/AhR-YFP, 100 ng of pGudLuc6.1, 100 ng of pSV- $\beta$ -galactosidase, and equalized to 1.5  $\mu$ g of total DNA with 1.25  $\mu$ g of pcDNA3. Control transfections contained 100 ng of pGudLuc6.1, 100 ng of pSV- $\beta$ -galactosidase, and were equalized to 1.5  $\mu$ g of total DNA with 1.3  $\mu$ g of pcDNA3. Twenty-four hours after transfection, cells were then incubated with either DMSO (1  $\mu$ L/ml) or 10 nM TCDD (1  $\mu$ L/ml) for 8 h. At the end of the exposure period, cells were lysed and assayed for luciferase activity. Luciferase activity is expressed as RLUs and was normalized to  $\beta$ -galactosidase activity.

**Statistical Analysis.** Unless otherwise specified, mean values are reported as means  $\pm$  S.E.M. Analyses of variance (ANOVA) with Duncan's multiple range test were performed to test for differences between treatment groups ( $\alpha = 0.05$ ). A two-sided Student's *t* test was used to identify differences between subgroups within multiple treatments ( $\alpha = 0.05$ ). All statistical tests were performed with the Statistical Analysis System (SAS) version 6.0 on an IBM microcomputer.

## Results

**Sequence Analysis of AhR Mutants.** Automated DNA sequencing confirmed that only the selected base changes were made to the A78D, the F82A, and the double mutant F82A:A78D cDNAs. Sequence analysis also confirmed, as previously reported by Sun et al. (Sun et al., 1997), bases 221 and 222 for the murine AhR sequence in GenBank read GC rather than CG. Sun et al. (1997) noted that this would change an amino acid coding for threonine to serine at position 74. This base change was anticipated from this earlier reporting and was taken into account when mutagenesis primers were designed.

**Changing Conserved Residues within the Purported AhR TPR Half-Site Does not Significantly Influence hsp90 or XAP2 binding.** For the initial characterization of AhR mutants, we examined interprotein interactions between the AhR and its dimerization partners. These examinations included determining whether the mutant AhRs could form a complex with hsp90 and XAP2 as well as form a heterodimer with ARNT. The assessment of these interactions between the mutant AhR proteins, hsp90, and XAP2 were carried out by transiently transfecting COS-1 cells with either the wild-type AhR cDNA, or mutant AhR cDNAs, along with the XAP2 cDNA. Thirty-six hours after transfection, hsp90, and XAP2 were coimmunoprecipitated using an anti-AhR mAb. To show the specificity of this coimmunoprecipitation, COS-1 cells were transfected with pcDNA3 along with the XAP2 cDNA. The results from this control experi-

ment demonstrated the specificity of the mAb RPT9 for the AhR (Fig. 2, lane 1). Figure 2 (lanes 3 to 5) demonstrates that each mutant AhR protein interacts with hsp90 and XAP2 with an efficiency equal to the wild-type AhR (Fig. 2, lane 2).

**Heterodimerization Capability of AhR Mutants.** The ability of the wild-type AhR and mutant AhR proteins to dimerize with ARNT was assessed using an in vitro transcription-translation-coupled reticulocyte expression system. An equimolar amount of in vitro synthesized ARNT-FLAG (unlabeled) was mixed with equimolar amounts of [<sup>35</sup>S]methionine-labeled AhR proteins in the presence and absence of TCDD and incubated at 30°C for 2 h to permit heterodimerization. The amount of AhR protein that dimerized with ARNT/FLAG was determined by coimmunoprecipitation with anti-FLAG M2 affinity resin. The specificity of the coimmunoprecipitation assay was evaluated by using anti-Flag M2 affinity resin that was blocked with the FLAG peptide. Blocked M2 anti-FLAG affinity resin immunoprecipitated a minimal amount of ARNT-AhR complex. A small but detectable amount of wild-type AhR and mutant AhR proteins coimmunoprecipitated with ARNT/FLAG in the absence of TCDD (Fig. 3A, lane 1). The amount of AhR coimmunoprecipitated with ARNT/FLAG was significantly increased for all AhR cDNAs in the presence of TCDD (Fig. 3A, lanes 3, 5, 7, and 9). Figure 3B represents a summary of the dimerization activity of each mutant AhR protein in the presence and absence of TCDD relative to wild-type AhR from three independent experiments. Under these experimental conditions, there was a small but insignificant decrease in the ability of A78D, F82A, and A78D:F82A to dimerize with ARNT relative to the wild-type AhR, as well as a small but insignificant increase in AhR-ARNT dimerization in the absence of TCDD. The marginal differences in dimerization levels for the mutant AhRs in the presence and absence of TCDD is not believed to result from a difference in the coupled-transcriptional-translational efficiency of the mutant AhR cDNAs. Figure 3C illustrates approximately equal expression efficiency for each of the AhR cDNAs in the reticulocyte system.

**Functionality of Mutant AhR cDNAs Expressed in cell Lines.** COS-1 cells and BP8 cells were used to test the functionality of the mutant AhR constructs. COS-1 cells were

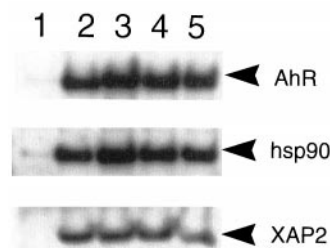


**Fig. 2.** AhR mutants retain the ability to bind hsp90 and XAP2. COS-1 cells were transfected in 10-cm<sup>2</sup> plates with either 6  $\mu$ g of wild-type pcDNA3/ $\beta$ AhR or mutant pcDNA3/ $\beta$ AhR and 3  $\mu$ g of pCI/XAP2 or with 6  $\mu$ g of empty pcDNA3 vector and 3  $\mu$ g of empty pCI vector. Thirty-six hours after transfection, AhR-hsp90-XAP2 complexes were immunoprecipitated with mAb RPT9. Blots were probed with mAb RPT1, anti-hsp84/86 rabbit polyclonal antibodies, and anti-XAP2 rabbit polyclonal antibodies. Bound antibodies were detected with either <sup>125</sup>I-sheep-anti-mouse IgG or <sup>125</sup>I-donkey-anti-rabbit IgG. Lane 1 demonstrates the specificity of the mAb RPT9 for the AhR as well as background binding by the use of anti-mouse IgG agarose not bound to mAb RPT9. Lanes 2, 3, 4, and 5 demonstrate that the wild-type AhR, A78D, F82A, and A78D:F82A, respectively, each interact with hsp90 and XAP2 with an equal efficiency.

chosen because they express low levels of endogenous AhR (Fig. 4A, lane 9) and BP8 cells were chosen because they do not endogenously express AhR (Wiebel et al., 1991). Figure 4A (lanes 1–8) illustrates that each of the mutant AhR cDNAs are expressed at approximately equal levels in COS-1 cells when normalized against p50 levels. To analyze the biological functionality of the mutant AhR constructs, AhR cDNAs were cotransfected along with an XRE-driven expression vector and a  $\beta$ -galactosidase expression vector. The wild-type AhR cDNA and an empty vector were included as a positive and negative controls, respectively. The modest TCDD-dependent activation of XRE-driven luciferase reporter activity in COS-1 cells, which were not transfected with wild-type AhR, reflects the small amount of endogenous AhR expression (Fig. 4B). This modest level of induction (2-fold) was not detectable in BP8 cells because of their lack of endogenous AhR. Changing the uncharged alanine residue at position 78 to an aspartic acid (A78D) abolished TCDD-dependent AhR activation in both cell lines (Figs. 4B). How-

ever, the F82A mutation reduced basal activity to background levels and caused a reduction in induced luciferase activity in both cell lines of approximately 50%. Differences in absolute activity between the wild-type AhR and F82A are

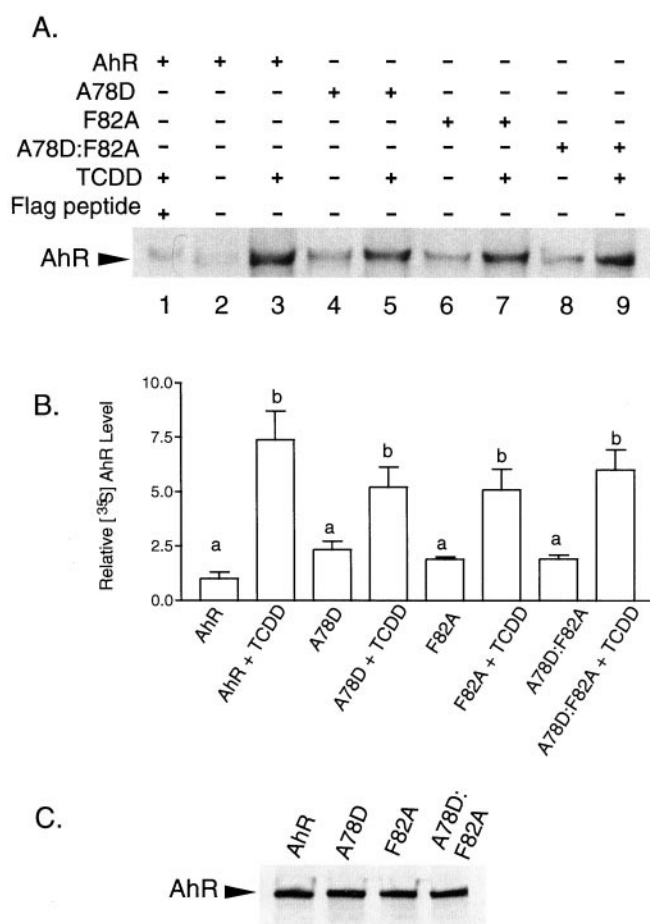


**Fig. 3.** AhR mutants retain the ability to heterodimerize with ARNT. A, ARNT heterodimerization activity of AhR mutants. Equal amounts of in vitro translated wild-type and mutant <sup>35</sup>S-AhR-labeled proteins were mixed with an equal amount of ARNT/Flag in the presence or absence of 20 nM TCDD. Anti-Flag M2 affinity resin was used to immunoprecipitate ARNT-<sup>35</sup>S-AhR and <sup>35</sup>S-AhR levels were quantified by PhosphorImaging. B, quantitative comparison of the results from three independent experiments that examined ARNT heterodimerization activity of wild-type AhR relative to AhR mutants. Values are presented as means  $\pm$  S.E.M. for three independent experiments. Bars with the same letter were not significantly different as determined with ANOVA and Duncan's multiple range test ( $\alpha = 0.05$ ).

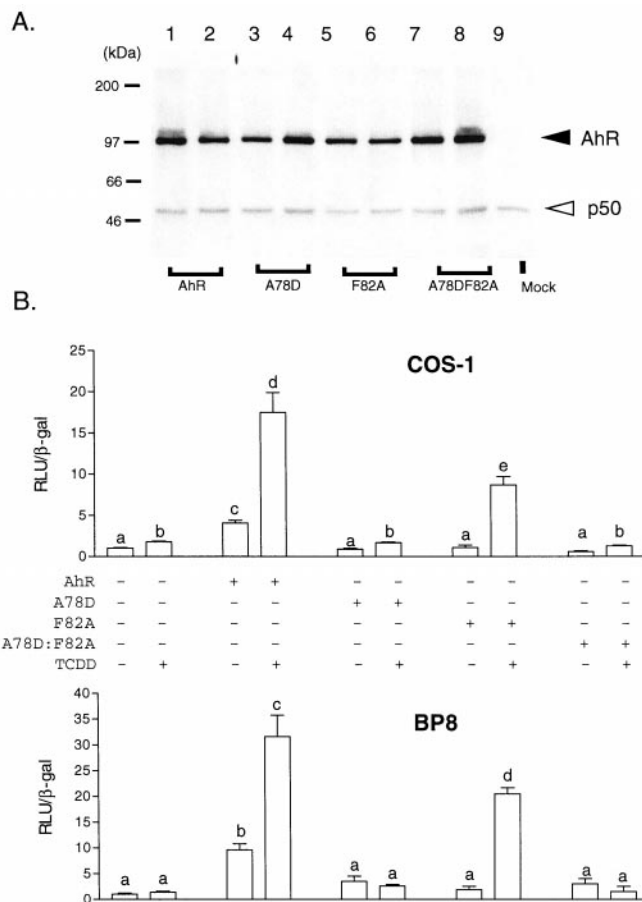


**Fig. 4.** Functionality of AhR mutants in COS-1 cells and BP-8 cells. A, quantitative Western blot of AhR expression levels in COS-1 cells. COS-1 cells were plated into 10-cm<sup>2</sup> culture dishes (80% confluent) and transfected with 0.5  $\mu$ g of either wild-type or mutant pcDNA3/ $\beta$ mAHR cDNA constructs and 8.5  $\mu$ g of pcDNA3 or with 9  $\mu$ g of cDNA3 as a mock transfection. One hundred micrograms of COS-1 cytosol from transfected cells was resolved by SDS-PAGE on an 8% Tricine gel and transferred to a PVDF membrane. AhR was detected with mAb RPT1 and AhR levels were normalized to p50 levels by probing with the anti-p50 mAb C1p50. Antibodies were detected with <sup>125</sup>I-sheep anti-mouse IgG and AhR and p50 levels were measured by PhosphorImaging. Lanes 1 and 2 represent the wild-type AhR; lanes 3 and 4 represent the A78D mutant; lanes 5 and 6 represent the F82A mutant; lanes 7 to 8 represent the A78D:F82A mutant, and lane 9 represent the mock transfection. B, xenobiotic response element reporter activity of COS-1 and BP8 cells transfected with either the wild-type AhR cDNA or mutant AhR cDNAs. COS-1 cells were grown in six-well dishes and cotransfected with 50 ng of either wild type pcDNA3/ $\beta$ mAHR or mutant pcDNA3/ $\beta$ mAHR, 100 ng of pGudLuc6.1, 100 ng of pSV- $\beta$ -galactosidase, and equalized to 1.5  $\mu$ g of total DNA with 1.25  $\mu$ g of pcDNA3. BP8 cells were grown in six-well dishes and cotransfected with 50 ng of either wild type AhR or mutant AhR, 100 ng of pGudLuc6.1, and equalized to 1.5  $\mu$ g of total DNA with 1.35  $\mu$ g of pcDNA3. Twenty-four hours after transfection, cells were incubated with either DMSO or 10 nM TCDD for 8 h and then cell lysates were prepared. Luciferase activity was determined from cell lysates and is expressed as relative light units (RLU). Luciferase activity for COS-1 cells was normalized to  $\beta$ -galactosidase activity and AhR expression levels measured in COS-1 cells calculated from the quantitative Western blot in A. Luciferase activity for BP8 cells was normalized to total protein levels. Transfection groups are presented as means  $\pm$  S.E.M. ( $n = 6$ ). Bars with the same letter were not significantly different, as determined with ANOVA and Duncan's multiple range test ( $\alpha = 0.05$ ).

not believed to result from differences in expression, because each of the AhRs are expressed at similar levels in COS-1 cells.

To uncover the mechanism that prevented the A78D from inducing XRE reporter gene activity, the capacity for each mutant AhR-ARNT dimer to bind to a  $^{32}$ P-labeled XRE sequence was analyzed. In vitro, AhR and ARNT proteins were synthesized in the absence of  $^{35}$ S-labeled methionine, mixed in equimolar ratio, and incubated either in the presence or absence of 20 nM TCDD. Formation of the AhR-ARNT-XRE complex was detected with a gel mobility shift assay. As a negative control, AhR alone was used to demonstrate the specificity of the AhR-ARNT heterodimer to bind the XRE consensus sequence (Fig. 5, lane 3). With this in vitro assay, the A78D mutation had significantly reduced XRE binding in the presence of TCDD (Fig. 5, compare lanes 2 and 5 with lanes 5 and 9). There was an approximately 60–80% reduction in AhR-ARNT-XRE binding by TCDD-activated AhR proteins that contained the A78D mutation. Although there was a 60–80% reduction for the two AhR proteins that contained the A78D mutation, there was a significant increase in XRE binding in the presence of TCDD relative to parallel

non-TCDD activated samples. The results from this in vitro DNA binding analysis, implicate the disruption of XRE binding as the primary mechanism for abolishing XRE-driven gene activity by the A78D mutation and support the results from transient transfection in COS-1 cells and BP8 cells. In contrast to the A78D mutation, the F82A mutation did not reduce in vitro XRE binding.

Additionally, the mutations introduced into the AhR sequence could have influenced the ability of the mutant AhRs to translocate to the nucleus after ligand activation. To assess whether the A78D or the F82A mutation modulated TCDD-dependent translocation to the nucleus, the A78D or the F82A mutations were placed into a murine AhR cDNA fused with a yellow fluorescent cDNA (AhR-YFP) (Petrulis et al., 2000). For this analysis, XAP2 was cotransfected with the AhR into the COS-1 cells. Cotransfection of XAP2 is required for cytoplasmic compartmentalization of the AhR in COS-1 cells. Previous work in our laboratory demonstrated that an AhR:XAP2 ratio of 1:2 is adequate for cytoplasmic compartmentalization of the inactivated AhR in transfection experiments and permits TCDD-dependent translocation of the AhR-YFP into the nucleus of COS-1 cells (Petrulis et al., 2000). In a similar study, LaPres et al. (2000) demonstrated with immunocytochemistry in COS-1 cells that ARA9, a homolog of XAP2, is also required for cytoplasmic localization of the inactivated AhR in AhR-transfected COS-1 cells. Furthermore, it has been shown that the AhR-YFP protein is able to associate with hsp90 and XAP2 in a capacity similar to that of the wild-type AhR (Petrulis et al., 2000). Based on the results of these two studies, a 1:2 (AhR:XAP2) ratio was chosen to characterize nuclear translocation of the mutant AhR-YFP proteins (Petrulis et al., 2000). In the present study, results from translocation experiments in COS-1 cells demonstrated that the wild-type AhR-YFP protein and the mutant AhR-YFP proteins can translocate to the nucleus after a 1-h exposure to 10 nM TCDD. Figure 6A illustrates a defined translocation of each AhR-YFP construct from the cytoplasm into the nucleus after TCDD treatment. Additionally, each of the AhR-YFP proteins were tested for their ability to activate XRE driven luciferase activity in COS-1 cells. The results from this AhR activation study were similar to results previously reported for the wild-type AhR and the mutant AhR proteins in COS-1 cells (Fig. 4B). As with the pcDNA3/ $\beta$ mAHR cDNAs, the wild-type AhR-YFP construct was capable of activating XRE-driven reporter activity in the presence of 10 nM TCDD in COS-1 cells (Fig. 6B). Also, as described for the nonYFP AhR cDNAs, AhR-YFP mutants that contained the A78D mutation were unable to activate XRE-driven luciferase activity and the F82A mutation had a reduction of roughly 50% in induced luciferase activity in the presence of TCDD.

## Discussion

A search of the murine and human AhR protein sequences for a putative TPR domain identified a partial TPR site. An amino acid sequence extending from the carboxyl-terminal end of the HLH region contains the conserved residues for domain B of the consensus TPR sequence. This domain is found in the murine and human AhRs between amino acids 78 and 90. Amino acids 78 to 90 were predicted to form an  $\alpha$ -helix as determined by the Chou-Fasman analysis (Chou

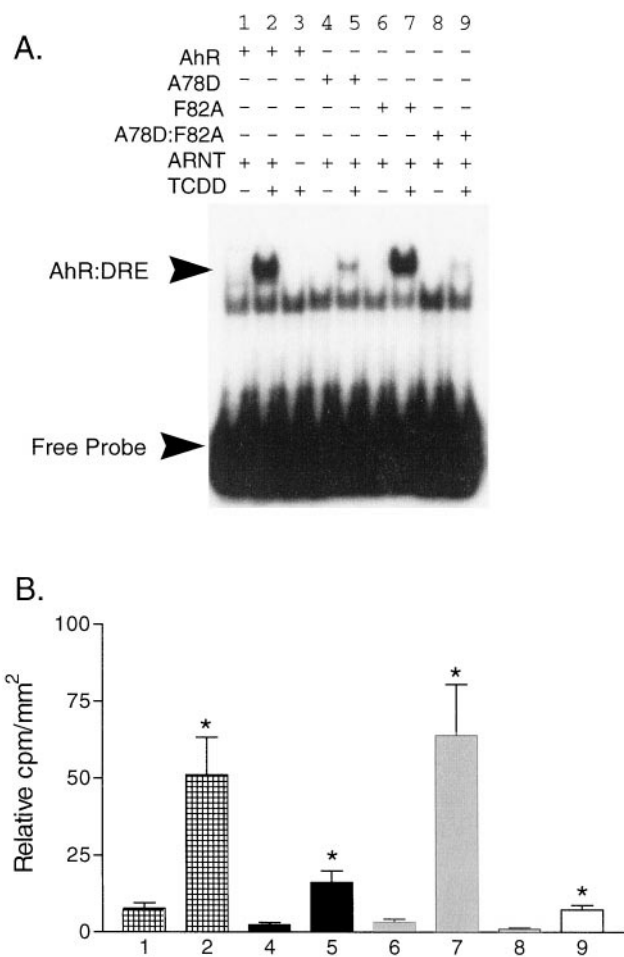


**Fig. 5.** DNA binding activity of AhR mutants. A, equal amounts of in vitro transcribed/translated AhR and ARNT were mixed together and analyzed for their XRE binding activity. B, summary of values and statistical comparison of values from gel shift experiments. The numbers below each bar correspond to the lane assignments from part A. Groups are presented as means  $\pm$  S.E.M. ( $n = 4$ ) and statistical comparisons were done with the Student's  $t$  test ( $\alpha = 0.05$ ). Bars with an asterisk were determined to be significantly different from their respective controls, which did not receive TCDD.



and Fasman, 1978) and the Garnier-Robson technique (Garnier et al., 1978). In addition, the Eisenberg hydrophobic moment method predicts that this region is an amphipathic  $\alpha$ -helix. The  $\alpha$ -helical structure of this region is consistent with the previous characterization of domain B of TPRs (Lamb et al., 1995). Site-directed mutagenesis of two conserved residues within this region was carried out to examine the possibility that this purported TPR half-site can modulate AhR functionality. Previously, investigations in our laboratory examined the functional importance of the TPR domain within the carboxyl-terminus of XAP2. This investigation demonstrated that deletion of either the carboxyl-terminus of XAP2 or selective mutations to conserved TPR residues can block interaction with AhR and hsp90 (Meyer et al., 2000).

Changing the conserved glycine residue at position 272, in domain A of the XAP2 TPR, to either a glutamic acid or aspartic acid, abolished XAP2 binding with AhR-hsp90 complexes in COS-1 cells. This same domain A mutation, in the TPR of *Saccharomyces cerevisiae* and a human homolog, results in a loss-of-function phenotype (Sikorski et al., 1993). Additional mutations of the XAP2 TPR, which included changing the tyrosine in domain A to an alanine, the amino-terminal alanine in domain B to a threonine, and the phenylalanine in domain B to an alanine, did not influence the interaction between XAP2 and AhR-hsp90 complexes in COS-1 cells.

To examine the potential functional role of the purported TPR half-site within the AhR, amino acid changes were chosen that could significantly alter the predicted  $\alpha$ -helical structure of this region. The first modification substituted the neutral alanine residue at position 78 with a charged aspartic acid residue (A78D). The second modification substituted the bulky side chain phenylalanine residue at position 82 with a nonbulky methyl side-chain alanine residue (F82A). A third mutant contained both substitutions (A78D:F82A). Because TPR domains have been shown to be important for intraprotein interactions and may be important in interprotein interactions, we hypothesized that selected changes to this region of the AhR could modulate interactions between the AhR and either XAP2, hsp90, or ARNT. The ability of the wild-type AhR and mutant AhRs to bind hsp90 and XAP2 was assessed in COS-1 cells, and the ability of the wild-type AhR and mutant AhRs to interact with ARNT was assessed with in vitro translated cDNAs. Collectively, the results from these coimmunoprecipitation experiments demonstrated that the A78D and the F82A mutations do not disrupt AhR interactions with either XAP2, hsp90, or ARNT.

Functional analysis of the mutant AhR constructs was tested in two cell lines, COS-1 cells, and BP8 cells. COS-1 cells and BP8 cells were satisfactory for this functional analysis, because COS-1 cells express low levels of endogenous AhR, and BP8 cells do not endogenously express AhR (Wiebel et al., 1991). Results from this analysis demonstrated that the A78D mutant completely abolished TCDD-dependent induction of XRE-driven luciferase activity. In vitro DNA binding analysis demonstrated that the loss of functionality of the A78D mutant resulted from a significant decrease in this mutant's ability to bind the core XRE sequence in the in vitro DNA binding assay. Based on our experimental data, it is unclear whether the loss of *trans*-activation potential of the A78D mutant was caused by an alteration in polarity, an alteration in side-chain specificity, or a combination of these two alterations at amino acid position 78. In contrast to the results obtained with A78D, the F82A mutant was capable of inducing TCDD-dependent induction of XRE-driven luciferase activity. However, there was a reduction in TCDD-induced luciferase activity in COS-1 cells and BP8 cells of approximately 50%. Nevertheless, the F82A mutant retained the ability to bind the core XRE sequence in the in vitro DNA binding assay. This comparison between the in vitro results from the F82A mutant in the DNA binding assay and the results from induction assays emphasizes the importance of using both in vitro assays and in vivo assays to assess AhR functionality. Additional analyses illustrated that the A72D and F82A mutations do not compromise the TCDD-dependent translocation to the nucleus. Therefore, the mechanism

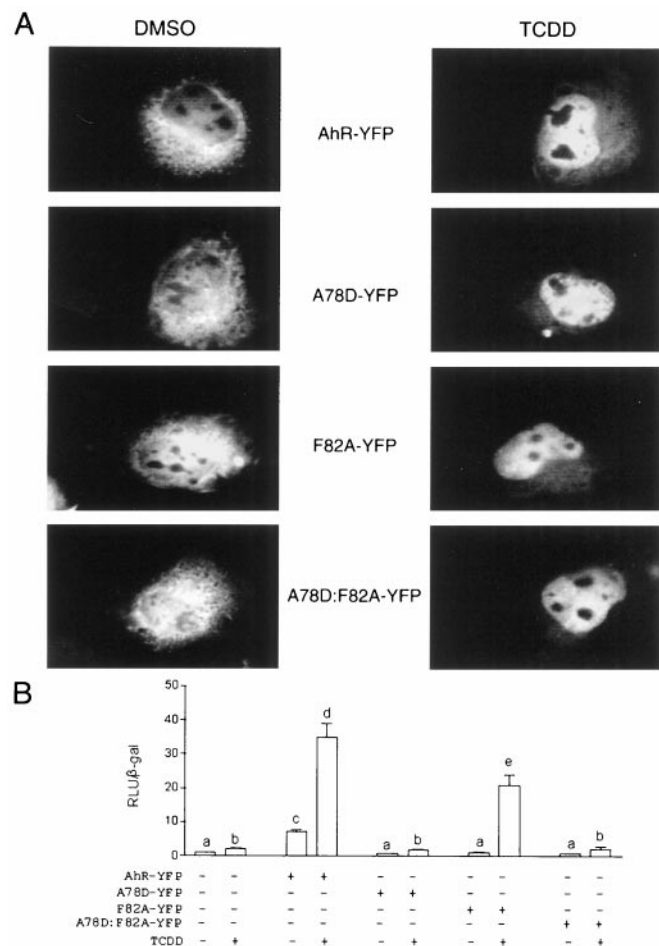


**Fig. 6.** TCDD-dependent *trans*-location of wild-type AhR-YFP and mutant AhR-YFP constructs. **A**, COS-1 cells were grown on glass coverslips in six-well culture dishes. Cells were transfected with 0.5  $\mu$ g AhR-YFP construct and 1.0  $\mu$ g pCI-XAP2 as described under *Experimental Procedures*. Cells were treated with either 10 nM TCDD or DMSO for 1 h before visualization by fluorescence microscopy. **B**, functionality of wild-type AhR and AhR-YFP mutants in COS-1 cells. COS-1 cells were seeded in six-well dishes and cotransfected with 50 ng of either wild type pcDNA3/ $\beta$ mAhR or mutant pcDNA3/ $\beta$ mAhR, 100 ng of pGudLuc6.1, 100 ng of pSV- $\beta$ -galactosidase and equalized to 1.5  $\mu$ g of total DNA with 1.25  $\mu$ g of pcDNA3. Twenty-four hours after transfection, cells were incubated with either DMSO or 10 nM TCDD for 8 h and cell lysates were prepared. Luciferase activity is expressed as relative light units (RLU) and normalized to  $\beta$ -galactosidase activity. Transfection groups are presented as means  $\pm$  S.E.M. ( $n = 3$ ). Bars with the same letter were not significantly different as determined with ANOVA and Duncan's multiple range test ( $\alpha = 0.05$ ).

underlying the difference in luciferase activity between the wild-type AhR and the F82A AhR is unclear. This reduction may reflect the existence of other proteins that influence the AhR-ARNT-XRE interaction in COS-1 and BP8 cells.

Previously, a mutant Hepa-1 cell line that was refractory to induction by PAHs and HAHs, was shown to contain a mutant form of the AhR (Sun et al., 1997). The cDNA for the mutant AhR derived from this cell line was shown to contain a C-to-G mutation at base 648 that caused a cysteine-to-tryptophan alteration at amino acid 216. Amino acid 216 (C216) is located in the PAS region between the PAS A and PAS B repeats. This mutation did not influence ligand binding or AhR-ARNT dimerization, but severely impaired XRE-binding. It was concluded that the loss of XRE binding by the mutant AhR resulted from either of two mechanisms. In the first mechanism, the mutation may have altered the tertiary structure of the AhR, thereby reducing DNA binding. In the second mechanism, C216 could be an important residue within a distal putative DNA binding domain. In a separate study, alanine scanning mutagenesis of the basic region of the murine AhR identified three residues that modulated DNA binding in vitro but only two residues that modulated *CYP1A1* expression in Hepa 1c1c7 cells (Dong et al., 1996). Dong et al. (1996) demonstrated that R14A, H38A, and R39A abolished XRE binding in vitro; however, H38A and R39A but not R14A were able to induce *CYP1A1* expression in Hepa 1c1c7 cells. Based on this finding, these authors also emphasized the importance of including both in vitro assays as well as cell line assays when screening the functionality of mutant AhRs. Contrary to our original hypothesis, the purported TPR half-site does not seem to influence protein-protein interactions between the AhR and known interacting partners. Rather, the A78D mutation influences DNA binding despite the fact that this mutation is adjacent to the HLH domain, which is distal to the basic region. Collectively, we conclude that selective changes to the amino-terminal sequence, outside of the basic region of the AhR, can affect XRE binding. Finally, these results underscore the potential importance of naturally occurring mutations to the AhR outside the basic region that may influence DNA binding.

#### Acknowledgments

We thank Marcia Perdew for valuable comments on this manuscript. We thank Mike Denison (Davis, CA) and Martin Gottlicher (Karlsruhe, Germany) for BP8 cells, Mike Denison for pGud Luc6.1, Steven Safe (College Station, TX) for TCDD, and Oliver Hankinson (Los Angeles, CA) for pcDNA3/βmAHR.

#### References

Burbach KM, Poland A and Bradfield CA (1992) Cloning of the Ah-receptor cDNA reveals a distinctive ligand-activated transcription factor. *Proc Natl Acad Sci USA* **89**:8185–8189.

Carver LA and Bradfield CA (1997) Ligand-dependent interaction of the aryl hydrocarbon receptor with a novel immunophilin homolog in vivo. *J Biol Chem* **272**:11452–11456.

Chou PY and Fasman GD (1978) Prediction of the secondary structure of proteins from their amino acid sequence. *Adv Enzymol* **47**:45–148.

Denison MS, Fisher JM and Whitlock JP (1988) Inducible, receptor-dependent protein-DNA interactions at a dioxin-responsive transcriptional. *Proc Natl Acad Sci USA* **85**:2528–2532.

Denison MS, Fisher JM and Whitlock JP (1989) Protein-DNA interactions at recognition sites for the dioxin-Ah receptor complex. *J Biol Chem* **264**:16478–16482.

Dolwick KM, Swanson HI and Bradfield CA (1993) In vitro analysis of Ah receptor domains involved in ligand-activated DNA recognition. *Proc Natl Acad Sci USA* **90**:8566–8570.

Dong L, Ma Q and Whitlock JP (1996) DNA binding by the heterodimeric Ah receptor. Relationship to dioxin-induced *CYP1A1* transcription in vivo. *J Biol Chem* **271**:7942–7948.

Eguchi H, Ikuta T, Tachibana T, Yoneda Y and Kawajiri K (1997) A nuclear localization signal of human aryl hydrocarbon receptor nuclear translocator/hypoxia-inducible factor 1beta is a novel bipartite type recognized by the two components of nuclear pore-targeting complex. *J Biol Chem* **272**:17640–17647.

Fukunaga BN and Hankinson O (1996) Identification of a novel domain in the aryl hydrocarbon receptor required for DNA binding. *J Biol Chem* **271**:3743–3749.

Fukunaga BN, Probst MR, Reisz-Porszasz S and Hankinson O (1995) Identification of functional domains of the aryl hydrocarbon receptor. *J Biol Chem* **270**:29270–29278.

Garnier J, Osguthorpe DJ and Robson B (1978) Analysis of the accuracy and implications of simple method for predicting the secondary structure of globular proteins. *J Mol Biol* **120**:97–120.

Goebel M and Yanagida M (1991) The TPR snap helix: A novel protein repeat motif from mitosis to transcription. *Trends Biochem Sci* **16**:173–177.

Hirano TN, Kinoshita N, Morikawa K and Yanagida M (1990) Snap helix with knob and hole: Essential repeats in *S. pombe* nuclear protein. *Cell* **60**:319–328.

Hord NG and Perdew GH (1994) Physicochemical and immunocytochemical analysis of the aryl hydrocarbon receptor nuclear translocator: Characterization of two monoclonal antibodies to the aryl hydrocarbon receptor nuclear translocator. *Mol Pharmacol* **46**:618–626.

Ikuta T, Eguchi H, Tachibana T, Yoneda Y and Kawajiri K (1998) Nuclear localization and export signals of the human aryl hydrocarbon receptor. *J Biol Chem* **273**:2895–2904.

Lamb JR, Michaud WA, Sikorski RS and Hieter PA (1994) Cdc16p, Cdc23p and Cdc27p form a complex essential for mitosis. *EMBO J* **13**:4321–4328.

Lamb JR, Tugendreich S and Hieter P (1995) Tetrapeptide repeat interactions: To TPR or not to TPR? *Trends Biochem Sci* **20**:257–259.

LaPres JJ, Glover E, Dunham EE, Bunker MK and Bradfield CA (2000) ARA9 modifies agonist signaling through an increase in cytosolic aryl hydrocarbon receptor. *J Biol Chem* **275**:6153–6159.

Ma Q and Whitlock JP (1997) A novel cytoplasmic protein that interacts with the Ah receptor, contains tetrapeptide repeat motifs, and augments the transcriptional response to 2,3,7,8-tetrachlorodibenzo-p-dioxin. *J Biol Chem* **272**:8878–8884.

Meyer BK and Perdew GH (1999) Characterization of the AhR-hsp90-XAP2 core complex and the role of the immunophilin-related protein XAP2 in AhR stabilization. *Biochemistry* **38**:8907–8917.

Meyer BK, Petrusis JR and Perdew GH (2000) Aryl hydrocarbon (Ah) receptor level are selectively modulated by the hsp90-associated immunophilin homolog XAP2. *Cell Stress Chaperones* **5**:243–254.

Meyer BK, Pray-Grant MG, Vanden Heuvel JP and Perdew GH (1998) Hepatitis B virus X-associated protein 2 is a subunit of the unliganded aryl hydrocarbon receptor core complex and exhibits transcriptional enhancer activity. *Mol Cell Biol* **18**:978–988.

Perdew GH (1988) Association of the Ah receptor with the 90-kDa heat shock protein. *J Biol Chem* **263**:13802–13805.

Perdew GH, Abbott B and Stanker LH (1995) Production and characterization of monoclonal antibodies directed against the Ah receptor. *Hybridoma* **14**:279–283.

Perdew GH, Bradfield CA (1996) Mapping the 90 kDa heat shock protein binding region of the Ah receptor. *Biochem Mol Biol Int* **39**:589–593.

Perdew GH, Hord N, Hollenback CE and Welsh MJ (1993) Localization and characterization of the 86- and 84-kDa heat shock proteins in Hepa 1c1c7 cells. *Exp Cell Res* **209**:350–356.

Perdew GH, Wiegand H, Vanden Heuvel JP, Mitchell C and Singh SS (1997) A 50 kilodalton protein associated with raf and pp60(v-src) protein kinases is a mammalian homolog of the cell cycle control protein cdc37. *Biochemistry* **36**:3600–3607.

Petrulis JR, Hord NG and Perdew GH (2000) Subcellular localization of the aryl hydrocarbon (Ah) receptor is modulated by the immunophilin homolog hepatitis virus x-associated protein 2. *J Biol Chem*, in press.

Reyes H, Reisz-Porszasz S and Hankinson O (1992) Identification of the Ah receptor nuclear translocator protein (Arnt) as a component of the DNA binding form of the Ah receptor. *Science (Wash DC)* **256**:1193–1195.

Schmidt JV, Su GH, Reddy JK, Simon MC and Bradfield CA (1996) Characterization of a murine AhR null allele: Involvement of the Ah receptor in hepatic growth and development. *Proc Natl Acad Sci U S A* **93**:6731–6736.

Sikorski RS, Michaud WA and Hieter P (1993) p62cdc23 of *Saccharomyces cerevisiae*: A nuclear tetrapeptide repeat protein with two mutable domains. *Mol Cell Biol* **13**:1212–1221.

Sogawa K, Iwabuchi K, Abe H and Fujii-Kuriyama Y (1995) Transcriptional activation domains of the Ah receptor and Ah receptor nuclear translocator. *J Cancer Res Clin Oncol* **121**:612–620.

Sun W, Zhang J and Hankinson O (1997) A mutation in the aryl hydrocarbon receptor (AHR) in a cultured mammalian cell line identifies a novel region of AHR that affects DNA binding. *J Biol Chem* **272**:31845–31854.

Tsai JC and Perdew GH (1997) Ah receptor nuclear translocator protein heterogeneity is altered after heterodimerization with the Ah receptor. *Biochemistry* **36**:9066–9072.

Whitelaw ML, Gustafsson JA and Poellinger L (1994) Identification of transactivation and repression functions of the dioxin receptor and its basic helix-loop-helix/PAS partner factor Arnt: Inducible versus constitutive modes of regulation. *Mol Cell Biol* **14**:8343–8355.

Whitlock JP (1987) The regulation of gene expression by 2,3,7,8-tetrachlorodibenzo-p-dioxin. *Pharmacol Rev* **39**:147–161.

Wiel FJ, Klose U, Kiefer F and Gottlicher M (1991) Toxicity of 2,3,7,8-tetrachlorodibenzo-p-dioxin in vitro: H4IIEC3-derived 5L hepatoma cells as a model system. *Toxicol Lett* **55**:161–169.

**Send reprint requests to:** Gary H. Perdew, Center for Molecular Toxicology and Carcinogenesis, Department of Veterinary Science, Pennsylvania State University, 226 Fenske Lab, University Park, Pennsylvania 16802